JTTEE5 13:274-282
DOI: 10.1361/10599630419427
1059-9630/$19.00 © ASM International

Peer Reviewed

Evaluation of Coatings Produced via Kinetic and Cold Spray Processes

T. Van Steenkiste and J.R. Smith

(Submitted 24 February 2003; in revised form 12 May 2003)

An analysis of physical and mechanical properties of coatings produced by kinetic and cold spray processes is presented. Adhesion, hardnesses, porosities, critical velocities, and other properties of aluminum and copper coatings from both spray methods are analyzed and discussed, including scanning electron microscopy and optical micrographs. Similarities and differences between each of the coating methods and their effects on the resulting coatings are presented. A brief history and discussion of the bonding mechanisms for the larger particle coatings produced by the kinetic spray method is provided.

Keywords coatings, cold spray, kinetic spray

1. Introduction

The first proposals in the patent literature for using the thermal and kinetic energies of high-velocity particles to make coatings that we are aware of are from Smith et.al.[1] Using the kinetic energy component only, Rocheville[2] used high-pressure air to make cold spray metallic and lubricating coatings. Browning[3,4] proposed injecting powder into high-velocity gases heated by an internal burner to a temperature below the powder melting point, providing enough velocity to achieve an impact energy transformation sufficient to raise the local coating temperature high enough to fuse the material into a dense coating.

Alkhimov, Papyrin, and coworkers developed a cold spray process at the Institute of Theoretical and Applied Mechanics of the Siberian Division of the Russian Academy of Science in Novosibirsk[5] to accelerate particles of diameter d in the range 1 μm ≤ d ≤ 50 μm to velocities on the order of 450-1000 m/s. During experiments designed to test high-speed re-entry vehicles, in a supersonic wind tunnel using metal tracer particles, it was observed that under certain conditions the metal tracer particle's behavior would transform from an eroding process to one of a rapid build-up of material on the targets. Alkhimov, Papyrin, and coworkers successfully developed the process to produce coatings.[6] This group was able to deposit coatings of a wide range of pure metals, metal alloys, polymers and composites on various substrates.

A pilot plant was built in Russia to coat steel pipe with aluminum (Al) and zinc at a rate of approximately 5 m^2/min., demonstrating the scale-up potential of the new process. Alkhimov, Papyrin, and their coworker's discovery was translated to English and published[5] in 1990 and a U.S. patent issued in 1994.[6,7]

Currently, research on the cold spray process has expanded into groups of researchers at several research centers around the world, including Sandia National Laboratories,[8-11] the Institute of Theoretical and Applied Mechanics of the Russian Academy of Science,[12-17] Pennsylvania State University,[18,19] the University of Bundeswehr, Germany,[20] the University of Ottawa, Canada,[21] and various companies such as ASB Industries.[22]

A high velocity coating machine, partially funded by the National Center for Manufacturing Science (NCMS), was built and installed at the General Motors Research Laboratories (GMR) in 1997. Equipment for data recording and devices for feedback control of the process variables were instrumented into this new machine. Such equipment is important[8] in understanding the mechanism by which coatings are formed from solid particles impacting a substrate.[26]

Later it was discovered[23-25,28] that a new nozzle configuration allowed one to make coatings from powder particles of diameters larger than 50 μm and as large as 200 μm. We found this coating process for the larger particles (d > 50 μm) to be fundamentally different from that for smaller particles. For example, the mean critical velocity (velocity above which the coatings start to form) for our Al powder (D_{50} approximately 65 μm) was found[25] to be about 440 m/s as compared with mean particle velocity of 630 m/s reported[5,6] for Al particles of average diameter 10 μm. An early study investigating the onset of Al coating formation[28] and scanning electron microscopy (SEM) cross sections and fracture photos of the coatings show that the coatings consisted primarily of large diameter (greater than 50 μm) particles. We named this new process kinetic spray after the primary energy source in the process.

In both cold spray and kinetic spray, the powder feedstock is neither melted nor thermally softened prior to impingement onto the substrate. The conversion of the particle's kinetic energy to thermal and strain energies upon striking the substrate leads to a relatively adherent, low-porosity coating. The low temperatures involved in the coating processes produce coatings with relatively low oxide content and low thermal stress. Moreover, due to the low temperatures, phases present in the initial powder are retained in the coating.

Larger diameter powder particles provide several potential mechanical and economical advantages compared with smaller diameter (less than 50 μm) powders. There are also safety advantages. Explosiveness, minimum energy for ignition, and rate

T. Van Steenkiste and **J.R. Smith,** Delphi Research Laboratories, Shelby Township, MI 48315. Contact e-mail: Thomas.van.steenkiste@delphi.com.

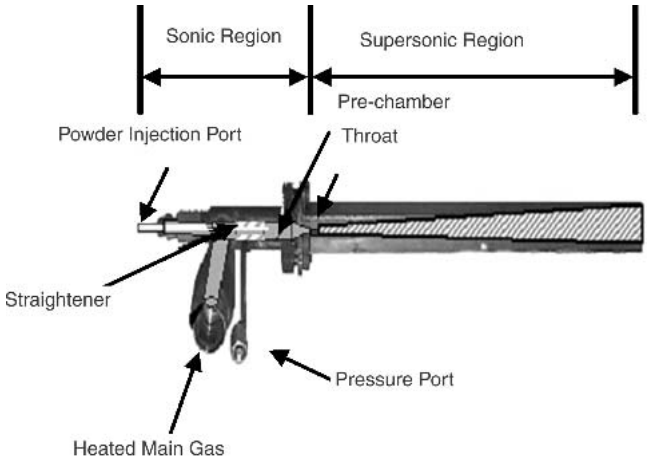

Fig. 1 Close-up diagram of the nozzle components

of pressure rise upon ignition[27] all decrease as the particle diameter increases. Moreover, health risks decrease as powder particle sizes increase because the human body has mechanisms to safely remove larger size particles. Supplier costs for larger diameter (greater than 50 μm) powders are usually lower than for smaller diameter (less than 50 μm) powder size distributions. These incentives lead the drive to discover a method for modifying the cold spray process to allow for the spraying of coatings from powder feed stocks greater than 50 μm in diameter. As will be described below, unexpected advantages in higher deposition efficiencies and lower critical velocities also accrue.

Both kinetic spray[23-25,28] and cold spray processes[1-22,26] have been described in detail in the literature. A review of the most important features follows. The kinetic spray and cold spray processes use a de Laval-type of nozzle to entrain metal powders in a supersonic airflow. A schematic diagram of the kinetic spray machine's nozzle components are shown in Fig. 1. A typical cold spray nozzle is similar in design and construction.

The speed of sound in a gas is dependent on both the gas temperature and the molecular weight of the gas. The equation for the speed of sound υ is

$$v = (\gamma R T / M_w)^{1/2} \quad \text{(Eq 1)}$$

where γ is the ratio of specific heats (1.4 for air, 1.66 for He), R is the gas constant (8314 J/kmol K), T is gas temperature, and M_w is the molecular weight of the gas. A convenient way to increase particle velocity (i.e., to increase the sound velocity), is to increase the main gas temperature or to use a lower molecular weight gas, such as helium (He). Increasing the pressure does not result in an increase in gas velocity upstream of the throat for the following reason. Once the pressure downstream is equal to 52.8% of the pressure upstream (for air), the flow through the nozzle throat becomes sonic. When the air velocity becomes sonic, further increases in the upstream pressure do not cause a further increase in the gas velocity through the nozzle throat (the flow is choked). Increasing the upstream pressure increases the density of the gas. Since the mass flow rate is also a function of density, the mass flow rate increases linearly with pressure while the gas velocity is constant. An increase in upstream pressure can also affect the drag coupling between the particles and the high velocity gas stream (changing the particle's velocity) as the drag properties are a weak function of the gas density. For the experiments in this report the main gas used was air in all cases.

Table 1 Comparison of the Original Alkimov, Papyrin Cold Spray Machine and the Kinetic Spray Machine

Parameters	Cold Spray Machine	Kinetic Spray Machine
Nozzle mach #	1.5-2.6	2.65
Gas pressure	0.51-1.0 MPa	2.0 MPa
Gas temperature	30-400 °C	204-650 °C
Working gas	air	air
Gas flow rate	18-20 g/s	18 g/s
Powder gas flow rate	0.1-10 g/s	1 g/s
Particle range	1-50 μm	65-200 μm
Ratio cross-sectional area of main gas to powder injector	49	126-388
Pressure differential (main gas/powder feeder gas)	0.17 MPa	0.17 MPa

Experiments to extend the spray parameter envelope (maximizing the main gas temperatures, changing to He as the main gas, maximizing the main gas pressures etc.), of the GMR/NCMS machine were unsuccessful in producing > 50 μm particle diameter coatings until we decreased the cross-sectional area of the powder feed injector in the main nozzle. The powder feed injection port (Fig. 1) is the device located in the prechamber of the nozzle that allows for a mixture of gas/particles to be injected into the main gas stream. This gas/particle stream is always at a slightly higher pressure than the main gas flow to ensure flow into the nozzle. When the powder feed injector tube was modified to have a cross-sectional area ratio (main gas /powder feed injector diameter) above 50, we started to produce coatings with larger diameter powders.[23-25,28] Table 1 is a comparison between the basic parameters of the kinetic spray machine[23-25,28] and the parameters of the original cold spray machine (the latter from the patent[6]).

Interestingly enough, it was also discovered[23,25] that it was possible to spray powders below 50 μm with a higher deposition efficiency using the smaller injector diameters. One might presume that the main effect resulting from the smaller injectors might be a reduced influx of cooler gas into the main gas stream. This cooler gas reduces the overall average main gas temperature resulting in a lower gas velocity with subsequent reduction in particle velocities. Calculations have indicated that the larger injector would lower the main gas temperature by several tens of degrees Celsius. However, if this were the only effect, then an increase in the main gas temperature by that amount should compensate for the cooling effect, all other parameters constant. We did not observe this to be true. Increasing the main gas temperatures did not allow for coating formation when spraying the larger particles.

The calculations also show that when the fixed pressure differential between powder carrier gas flow and main gas flow is maintained, the smaller injector would have an increased gas velocity and correspondingly higher initial particle velocity, prior to injection into the main gas flow in the prechamber. An estimate for the maximum increase in the particle velocity is 40-50 m/s before leaving the exit of the powder feeder injection tube.

This might be significant if one were near the mean critical

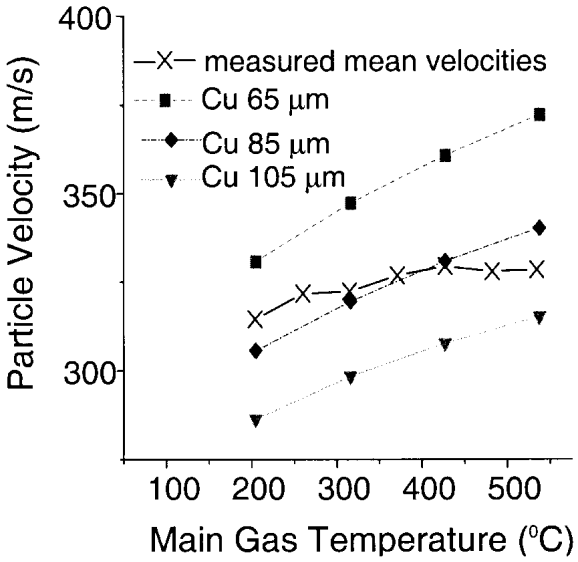

Fig. 2 Particle velocity measurements for Cu; computational and experimental (x) results are plotted.

velocity for coating formation,[6,8,23-26,28] while simultaneously at the upper limit of the spray apparatus's heating range. However, this was found not to be true for the materials tested. Again this effect should be overcome with the larger injector by increasing the main gas temperature. This was not to be the case. A discussion of these results as well as the possible reasons for the increased deposition probabilities for coatings of $d < 50$ μm particles and the enabling of coatings of particles of $d > 50$ μm follows later.

The curves marked with solid symbols in Fig. 2 result from a one-dimensional computation of the velocities of the main air and the particles assuming main air temperatures ranging from 200 to 527 °C, inlet pressure of the main air to be 2.0 MPa (300 psi), and relatively large diameter copper (Cu) powders (65-106 μm). Analytic equations were used to compute the gas velocities and temperatures in the nozzle from the gas inlet conditions and the nozzle area versus length.[25] Particle velocities in the nozzle were calculated from the drag forces using correlations in the literature.[29-31] Mean Cu powder velocities were measured with a laser two-focus velocimeter (Control Vision) at a point 5 mm from the exit of the nozzle and are also plotted in Fig. 2 as a function of main gas temperature shown as the curve marked with *x*'s. That the measured mean particle velocities do not increase as rapidly with main gas temperature as do the computed velocities is likely a result of the cooler powder feeder gas mixing with the main gas flow. One can understand this as follows. First, the powder feeder gas mass flow and density are constant (fixed pressure difference between the powder feeder and the main gas and the powder gas temperature fixed at room temperature). Secondly, with increasing main gas temperature *T,* the main gas density decreases as $1/T$. Thus the proportion of gas particles introduced at room temperature increases as T increases, consistent with a lower increase of particle velocity at the nozzle exit with increasing T. Future plans include moving the main gas thermocouple to the pre-chamber of the nozzle for accurate monitoring and computations of the influence of powder gas on particle velocities at the nozzle exit.

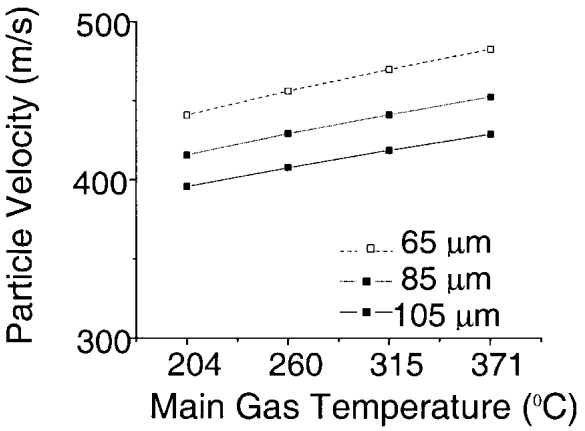

Fig. 3 Computed aluminum particle velocity (at nozzle exit) as a function of main air temperature

Computed particle velocities for Al particles in the size range and main air temperature range we sprayed are shown in Fig. 3. Note that in Fig. 2, 3, and 4, the particle velocities and particle temperatures are not nearly as sensitive to particle size as we found for smaller particles used in cold spray shown in Fig. 5. Secondly, note that the Al velocities are all substantially smaller than the mean critical velocity of about 630 m/s reported[5,6] for Al particles of average diameter equal to 10 μm. Here, the mean critical velocity is defined as that velocity above which coatings begin to form. We found that kinetically sprayed Al coatings began to form for a main gas temperature of 204 °C,[25,28] so that our Fig. 3 implies a mean critical velocity of about 440 m/s (for 65 μm particles). The Cu particle's mean velocity of 325 m/s (Fig. 2) is also lower than the mean Cu (again 10 μm average diameter) critical velocity reported by Alkimov et al.[5,6] of about 440 m/s. It is also lower than the 500 m/s reported by Gilmore et al. for 22 μm Cu particles (Fig. 9a in Gilmore et al.[10]).

Particle temperatures were calculated via a heat transfer correlation[25,26] (using the same conditions as in Fig. 3), and are shown in Fig. 4 and 5. These simple models, while ignoring boundary layer effects and heat transfer to the nozzle, do provide insight into the controlling factors of the particle velocities and temperatures. For small particles (less than 5 μm diameter) the response is very similar to that of the gas, while for larger particles (greater than 5 μm), a position dependent rise and fall of the temperature is noted.

Figures 5(a) and (b) provide calculated gas and particle velocities as a function of nozzle distance for various particle diameters. There is also a particle size dependence of the velocity distribution.[10,24-26,28]

An analysis of the mechanical and physical properties of several Al and Cu coatings (on brass substrates) produced using cold spray conditions as well as kinetic spray conditions was undertaken to determine if substantial differences exist in the coating processes.[26]

2. Experimental

The kinetic spray and cold spray processes use a de Laval-type of nozzle to entrain metal powders in a supersonic airflow.

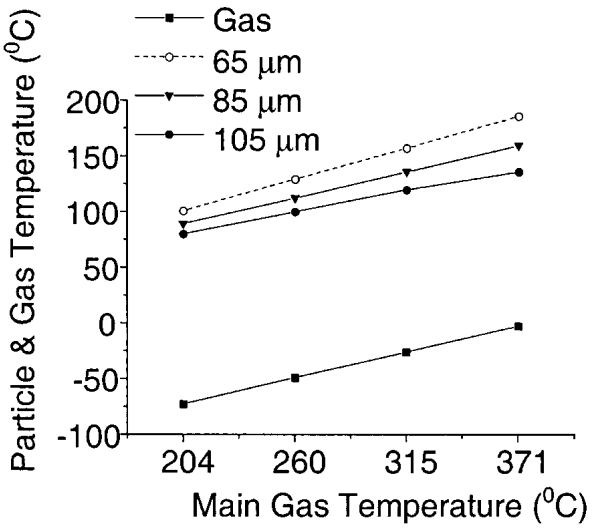

Fig. 4 Theoretical calculation of aluminum particle and gas temperatures (at nozzle exit) as a function of main gas temperature

A schematic diagram of the kinetic spray machine's nozzle components are shown in Fig. 1. A typical cold spray nozzle has similarities in design and construction. The nozzle has an entrance cone region with a diameter that decreases from 7.5 mm to a throat region of 2.8-3.0 mm diameter and is attached to an 84 mm long prechamber with an internal diameter of 19 mm on one end and 7.62 mm diameter on the nozzle attachment end. Downstream of the throat region, the nozzle has a rectangular cross section increasing to an exit of dimensions 10 mm by 2.8 mm. Figure 1 shows the location of the pressure sensor port and the main gas inlet thermocouple in the nozzle assembly. These sensors provide feedback for the computer control of the prechamber (before the throat) pressure and the inlet gas temperature. Similarly, the high-pressure powder feeder and feed rate of the incoming particles are monitored and computer controlled. The main gas temperature is varied by an in-line heater and is capable of heating the gas to 650 °C. The primary purpose of heating the main gas is to increase the sound velocity according to Eq 1.

The powder feed injection port (Fig. 1) provides a means for powder to be deposited into the high-velocity main gas flow. When we attempted to reproduce cold spray conditions, the powder injector had a diameter of 2.54 mm with a pressure differential of approximately 0.17MPa (25 psi) between the powder feeder and the main gas. This resulted in a powder gas flow rate of approximately 4 g/s. For our kinetic spray process, the injector has a diameter of 0.90 mm, a pressure differential of approximately 0.17MPa (25 psi) and a powder gas flow rate of approximately 1g/s.[23,24] Main air temperatures were 482 °C for the Cu coatings and 340 °C for the Al coatings.

The particle distributions (number %) for the Al and Cu powders are shown in Table 2 and were measured using a Mastersizer Microplus (Malvern Instruments, Southborough, MA).

Porosity measurements for the coatings were done with a He pycnometer (Micrometrics AccuPyc 1330, Norcross, GA). Samples were removed from their substrates, initially measured and then sealed with an anaerobic sealant (Loctite 990, Rocky Hill, CT) and the volume was measured again to determine open

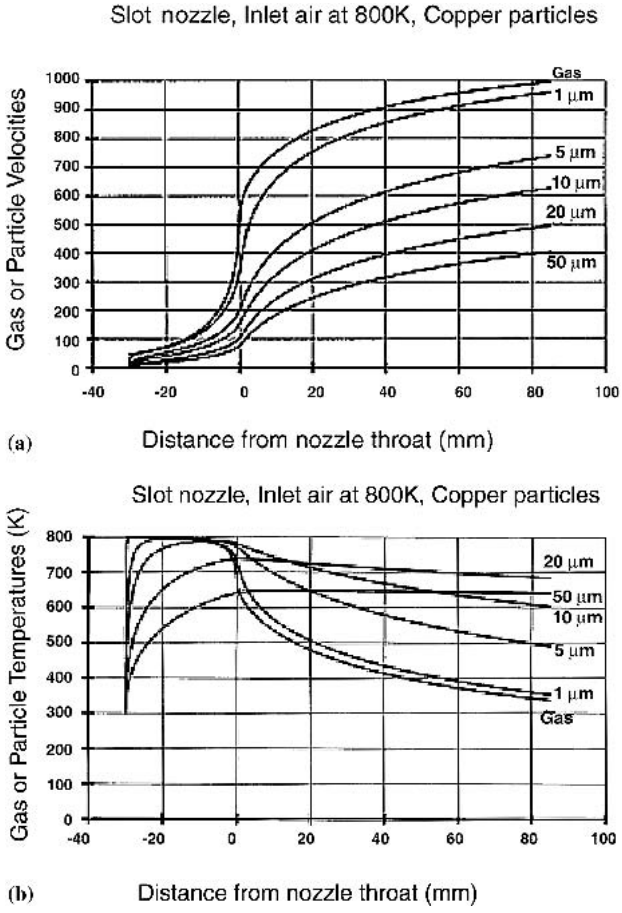

Fig. 5 **(a)** Computed air and particle velocities as function of distance along the nozzle. Particle diameters denoted in microns for the particle velocity curves.[25] **(b)** Computed air and particle temperatures as function of distance along the nozzle. Particle diameters are denoted in microns for the particle velocity curves.[25]

Table 2 Particle Size Distribution (Number %) for the Aluminum and Copper Powders

Material	Size Range	D10, μm	D50, μm	D90, μm
Al	Small	9	20	40
Al	Large	44.77	61.75	80.11
Cu	Small	(a)	(a)	(a)
Cu	Large	34	62	112

(a) These powders were not measured and were sieved to a −325 mesh (≤45 μm).

pore volume. Average coating thickness per single pass ranged from 1.5 mm (Cu cold spray] to 1.68 mm (Cu kinetic spray) and 0.4 mm (Al cold spray) to 0.7 mm (Al kinetic spray). Hardness measurements were made with a Matsuzawa Model MXT70-UL (Tokyo, Japan) ultra micro hardness tester. For each coating sample a series of 12 measurements were taken using a 1 g load. Results were averaged after removing the highest and lowest measured values. Adhesion measurements between the coating and the substrate were preceded by application of a South Bay Technologies Model 360 (San Clemente, CA) rotary disk cutter (using a silicon carbide slurry) or a laser to core a 2.97 mm di-

Table 3 Porosity, Adhesion, Cohesion, and Hardness Measurements for Kinetic and Cold Sprayed Al and Cu Coatings Produced Using Large (>50 μm) and Small (<50 μm) Diameter Particles With a Large Particle Feeder Injector of 2.54 mm Diameter and a Small Particle Feeder Injector of 0.9 mm Diameter

Method/Powder	Coating	Porosity, vol%	Hardness, HV	Adhesion, MPa (kpsi)
Cold spray, small particles	Cu(a)	4.49	95-113	26.2-44 (3.8-6.4)
Kinetic spray, large particles	Cu	2.1	51-98.7	28-50 (4.0-7.3)
Cold spray, small particles	Al(a)	3.72	34-51	33-35 (4.78-5.02)
Kinetic spray, large particles	Al(b)	1.75-4.51	48.7-52.3	21-68 (3-9.86)

(a) Ref 26
(b) Ref 25

ameter island thru the coatings to the substrate. Epoxy-coated pull studs (2.69 mm diameter) were bonded (1 h at 150 °C) to this island for testing using a Romulus IV adhesion testing machine (Quad Group, Spokane, WA). Unfortunately, the kinetically sprayed Al samples had been removed from their substrates[25] so that only cohesive tests could be performed. This was accomplished by bonding a stud to both sides of the Al coating and pulling until failure. Finally, deposition efficiencies were determined as the ratio of mass of the coating deposited on a large-area substrate to the mass of powder fed to the nozzle.

3. Results

Porosity measurements for the Al coatings produced using either cold spray or kinetic spray methods are shown in Table 3 and demonstrate a range of values between 1.75 and 4.51%. There is considerable overlap between porosities in the Al coatings produced with either method. The porosity of kinetically sprayed Cu is approximately half that of cold sprayed Cu, however. Hardness data for the various coatings is also displayed in Table 3. It was observed that the range of values for both large and small particles overlap with a suggestion that the hardness of the cold spray coatings are at the upper end of the range measured for the kinetic sprayed coatings for Cu, with the opposite result for Al. This difference in the hardness data is nearly within the scatter of the hardness measurements, however. Adhesion data for the two methods are comparable. In all cases, the adhesion failure mode was found to be within the coating. Note, as mentioned above, the adhesion data listed for the kinetically sprayed Al particles is actually cohesion data for the Al coating.[25]

The deposition efficiency for the kinetic spray method using both small and large diameter particles is shown in Fig. 6. Main air temperatures were 315 °C for Al and 482 °C for Cu coatings with a pressure differential of 0.17 MPa. Small and large diameter powder feeder injectors were used as well as several different powder feed rates. Looking at the Al coating results first, we note that coatings produced using the smaller diameter injector have deposition efficiencies ranging from 7% to 19%, for powders smaller than 50 μm (Fig. 6, open diamonds), while for the powders larger than 50 μm, the deposition efficiencies range from 20% to 45% (Fig. 6, filled diamonds). This is an increase of almost a factor of two.

Observing the Cu particle's response to injector size, we note that again larger diameter particles introduced via the smaller diameter injector have an improved deposition efficiency (70-75%; see Fig. 6, filled squares), by a factor of three in some cases, as compared with that of the smaller diameter particles (20-30%, open squares). The deposition efficiencies for coatings made from the small diameter particles and either powder feeder injector are comparable. Both range between approximately 20% and 30% (open squares and filled stars).

A 63.5 cm long prechamber (internal diameter 19 mm) was added before the nozzle in an effort to determine if potential turbulence near the throat due to the larger diameter injector (caused by the increased room temperature flow mixing with the 482 °C main airflow for Cu powders) could be overcome by a longer residence time, allowing for more time for any turbulence to subside before the mixed air flows entered the throat. Results for Cu coatings using the prechamber are plotted in Fig. 6 (open and filled circles). Note that the deposition efficiency for the larger particles using the smaller diameter injector has significantly dropped from the values measured previously without the prechamber. The deposition efficiencies are approaching those of the smaller diameter particles. The deposition efficiencies for the smaller diameter particles introduced via the larger diameter injector (cold spray method) are similar to those observed without the prechamber.

In Table 4, the oxygen concentration in the Cu coatings (weight percentas measured by Leco analysis), as a function of spraying parameters is shown with and without the prechamber. For the coatings sprayed using smaller diameter Cu particles (less than 50 μm) without the prechamber, there is little difference in the oxygen concentration: 0.18% (small injector) and 0.20% (large injector). With the prechamber attached, we observe an increase in the oxygen concentration in the coatings. The oxygen concentrations of the smaller injector coatings range from 0.44% to 0.53%, while the larger injector coatings range from 0.23% to 0.28%. The prechamber addition dramatically increased both residence times and particle temperatures, producing an increased oxidation of the particles. The larger diameter injector (with increased cooler gas flow) would appear to have an average prechamber particle temperature similar to the average particle temperature without the pre-chamber since the resulting oxygen concentration in the coatings is only slightly increased compared with the values measured for the coatings produced without the prechamber.

However, for the smaller diameter power feeder injector (with correspondingly smaller cooler gas flow, Table 1), an apparently higher average temperature of the combined gas mixture (main and powder feeder) could cause an increase in particle temperatures resulting in the increased oxidation levels mea-

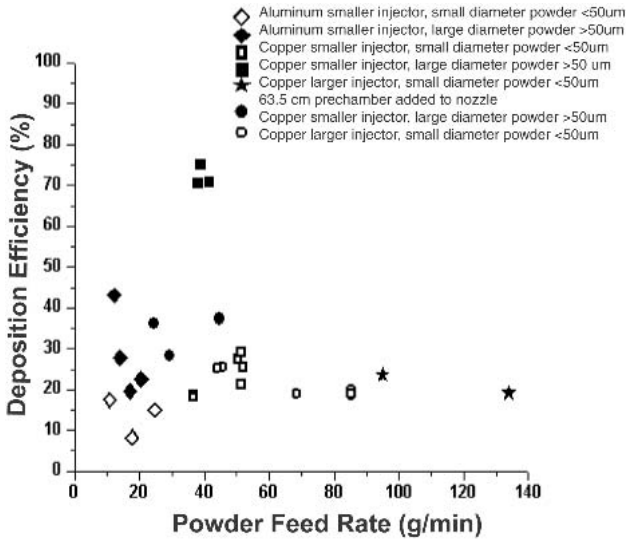

Fig. 6 Deposition efficiency plotted as a function of powder feed rate for various spraying conditions and powder feed injector diameters. The Al data were taken from the work of Ref. 25.

Table 4 Oxygen Concentrations of Cu Coatings Produced Using Smaller Diameter Particles With and Without the Addition of a Prechamber

Prechamber	Powder Feeder Injector Diameter, mm	Weight Percent Oxygen
No	0.9	0.18
No	2.55	0.20
Yes	0.9	0.44-0.53
Yes	2.55	0.23-0.28

sured in the coatings. Increased oxidation as a result of increased particle temperatures and mixing time can generate a thicker shell of oxide on the outer surface of the particle. This thicker oxide shell could frustrate plastic deformation of the particle upon collision with the substrate. Plastic deformation is necessary to convert the particle's kinetic energy to heat so that it can stick to the substrate. This perhaps explains why the prechamber deposition efficiencies for the smaller injector diameters (Fig. 6, open circles) are smaller than those with no prechamber (Fig. 6, open squares). In any case, there is certainly no evidence that adding the prechamber increases the deposition efficiency.

While the prechamber may decrease any turbulence due to mixing of the two gases at different temperatures, its effects seem to be masked by an increase in oxidation from the higher particle temperatures generated in the prechamber. Figures 7(a) and 7(b) contain SEM photos of an Al particle demonstrating the degree of plastic deformation that larger particles undergo in the kinetic spray process. Interestingly, one can observe the plastic flow of the grains near the impact site as well as the preservation of the original grain structure in locations removed from the impact site. Figure 8 is a SEM photo of the coating after fracturing. Note the flattening caused by multiple impacts with other particles (P's in photo) as well as the ductile fractures (D's in photo). Figure 9(a) is an optical photograph of a typical cold spray coating produced at 315 °C using smaller diameter (less

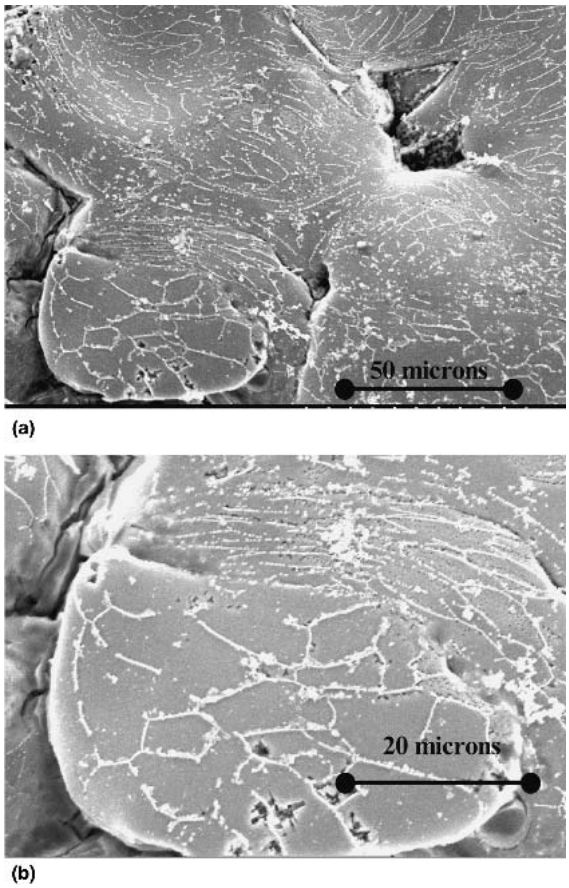

Fig. 7 **(a)** SEM image of an Al electro-polished coating cross section produced at main gas temperature of 260 C. **(b)** Magnified view of the electro-polished particle shown in the photo above. The plastic flow of the grains near the impact site and the preservation of the original grain structure in locations removed from the impact site are shown.

than 45 μm) particles with the larger diameter powder feeder injector. Figure 9(b) is an optical photograph of an etched kinetically sprayed Al coating produced at 315 °C using larger diameter particles and the smaller diameter powder feeder injector. Comparing Fig. 9(a) and 9(b), we observe plastic deformation of both the large diameter particles and the small diameter particles in the photos. From Table 3 the porosities and hardnesses of the measured coatings are comparable. Adhesion measurements on the kinetic and cold-sprayed Al coatings were also similar, with the same failure mechanism.

Figure 10(a) is an optical photo of an etched Cu coating from smaller diameter particles cold sprayed at 482 °C. Figure 10(b) is an optical photo of an etched Cu coating from larger diameter particles kinetically sprayed at 482 °C. Again, examination of the photos reveals the same basic high degree of plastic deformation and void reduction in the formation of the coatings. The porosity, adhesion, and hardness data from Table 2 for the kinetically and cold sprayed Cu coatings are again similar.

Figures 7, 9, and 10 all show the anisotropic nature of the coatings regardless of which process was used. This anisotropy results from the relatively large incident particle velocities (350-450 m/s, Fig. 3) for the kinetic sprayed coatings and the 630 m/s and higher mean values reported for smaller Al particles

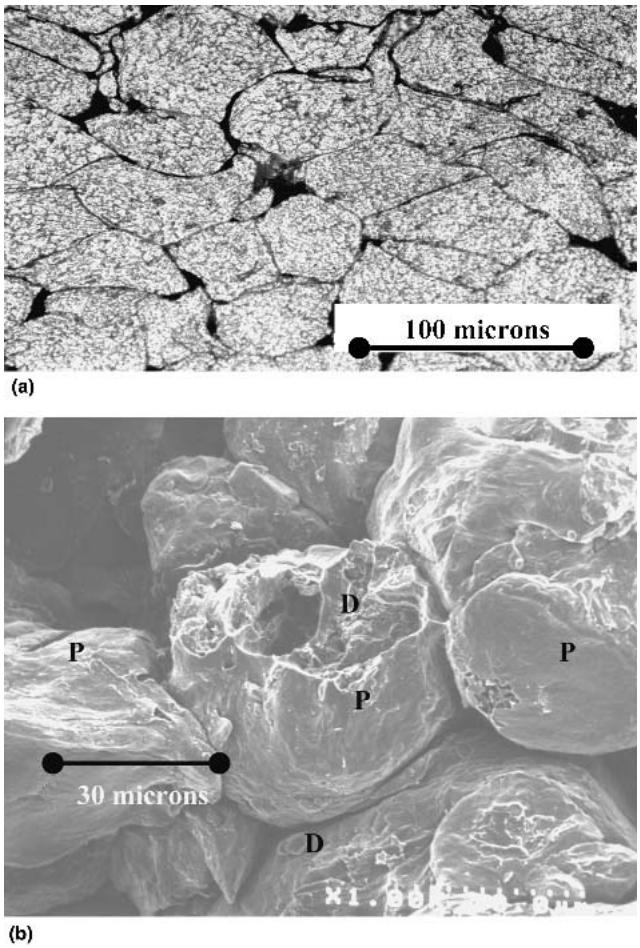

Fig. 8 SEM image of an Al coating fracture surface; P = flattening caused by particle impacts; D = ductile fracture

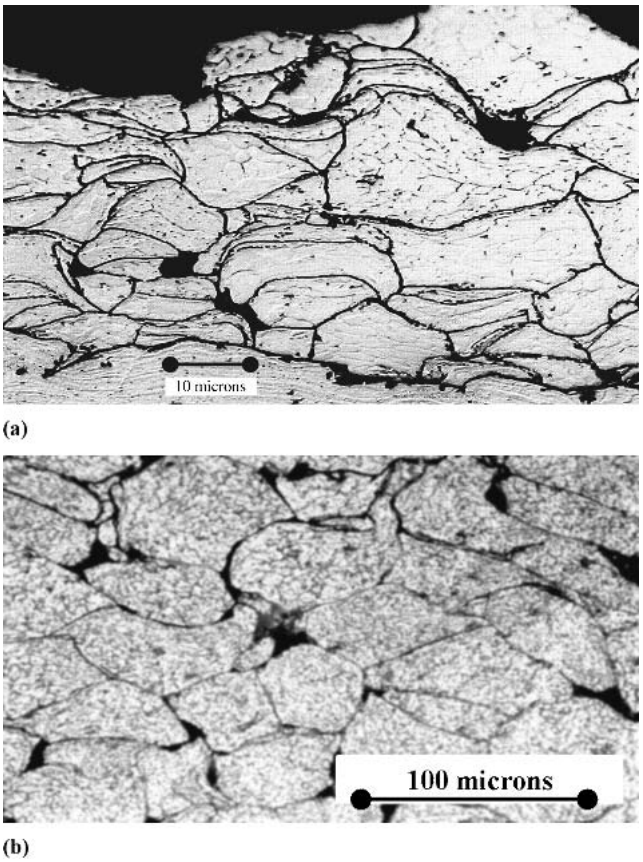

Fig. 9 **(a)** Optical photograph of the etched surface of a cold sprayed Al coating cross section (substrate located at bottom of picture) produced at a main gas temperature of 315 °C (600 °F). **(b)** Optical photograph of the etched surface of a kinetically sprayed Al coating cross section (substrate located at bottom of picture) produced at a main gas temperature of 315 °C (600 °F).

(~10 μm). The direction of these velocities is, to within the spread of the particle beam leaving the nozzle, perpendicular to the target surface (the axis of the nozzle also is perpendicular to the target surface). The roughly round powder particles are flattened, with their resulting larger dimensions parallel to the surface.

4. Discussion

How does one deal with the observation that mean critical velocities for the larger particles,[25,28] where the majority of the particles have diameters $d > 50$ μm, are substantially less than those reported for particles of average diameter 10 μm[5,6] or about 20 μm?[10] From Table 2, one can see that there is some overlap in the large and small powder size distributions. If one were to assume that the D_{10} particles of the large diameter powder distribution (which would be traveling the fastest) are the primary particles producing the coatings, one would observe in the fracture pictures and SEM cross sections primarily those particles. What is observed here and in previous experiments[25,28] is that large diameter particles of diameters substantially greater than 50 μm are primarily the particles producing the coatings. Figures 7, 8, and 9(b) clearly show the predominately large diameter particles in the coatings. The impact stress must exceed the yield stress for plastic deformation to occur, and plastic deformation is necessary for the particles to form coatings. Estimates for the impact stress $S \simeq \rho v^2/6$[25] hold no clue because S is approximately independent of d. For the particles to be involved in coating formation, there must be enough plastic deformation to convert all of the particle's kinetic energy ultimately into heat and strain energies. Perhaps the fact that the particles are not perfectly spherical plays a role. In that case, there will be instances where the contact point has a smaller radius of curvature than $d/2$, and the larger momentum of the larger particles could cause an impact stress to exceed the yield stress. Alternatively, perhaps the requirement of fracturing the particle oxide layer before plastic deformation can occur is important here. Again, the higher momentum of the larger particles could couple with a local small radius of curvature to create higher impact stress to fracture the oxide shell.

How does one understand the observations that the kinetic spray process parameters (Table 1) allow for deposition efficiencies of particles with $d > 50$ μm to be larger than those for $d < 50$ μm, while cold spray process parameters yield deposition efficiencies for $d > 50$ μm to be essentially zero? We have discussed

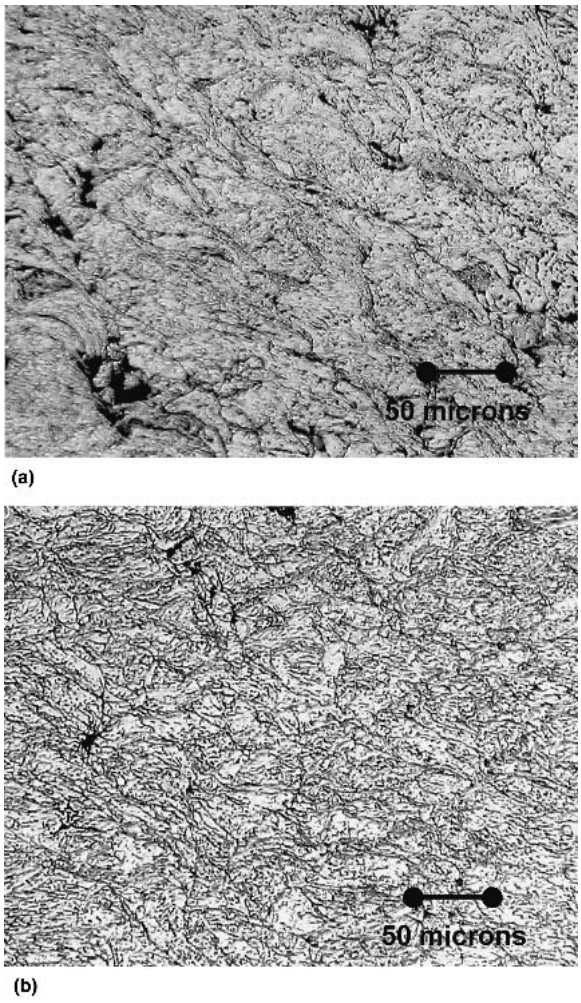

Fig. 10 **(a)** Cold sprayed Cu coating (less than 45 mm powder), at a 482 °C main gas temperature, substrate located at bottom of picture). **(b)** Kinetically sprayed Cu coating (greater than 63 mm powder), at a 482 °C main air temperature, and traverse speed of 6.4 mm/s (substrate located at bottom of picture).

above potentially lower net gas temperatures associated with larger injector tube diameters of cold spray but were unable to verify it as an explanation. Greater turbulence due to larger injection tube diameters may be a significant effect. Our attempt to modify the turbulence via a prechamber showed no apparent effect, suggesting that turbulence is not an important phenomenon. At this point, it is not clear why the smaller injector tube increases deposition efficiencies for larger particles. Also, there is currently no definitive answer to the physics behind the observation of a significant dependence of the critical velocity on particle diameter.

5. Summary

The kinetic spray process exhibits relatively high deposition efficiencies for particles as large as 200 μm, while the cold spray process is limited to particle diameters $d < 50$ μm. Mean critical velocities of the larger particles ($d > 50$ μm) are significantly smaller than those of the smaller particles ($d < 50$ μm). Process parameters of the two methods are compared, and the smaller powder injection tube diameters of the kinetic spray process appear to be the most important difference. Resulting higher gas temperatures and possibly lower turbulence upstream of the throat are kinetic spray properties discussed as potential explanations for observed differences between the kinetic and cold spray process properties.

Acknowledgments

The authors would like to acknowledge numerous useful conversations with Dr. Richard Teets, Dr. Alaa Elmoursi, Dr. Zhibo Zhao, Mr. Bryan Gillispie, and Mr. Nilesh Patel of Delphi Research Laboratories, as well as the assistance of Mr. Daniel Gorkiewicz in the spraying of the coatings. Dr. Taeyoung Haun is also acknowledged for the gas and particle velocities and temperature calculations.

References

1. G.H. Smith, N.Y. Kenmore, R.C. Eschenbach, and J.F. Pelton, U.S. Patent 2 861 900, Jet Plating of High Melting Point Materials (Nov. 25, 1958).
2. C.F. Rocheville, U.S. Patent 3 100 724, Device for Treating the Surface of a Workpiece (Aug. 13, 1963).
3. J.A. Browning: "What If We're Right?" *Thermal Spray*: *A United Forum for Scientific and Technological Advances,* C.C. Berndt, ed., ASM International, Materials Park, OH, 1997 pp. 15-18
4. J.A. Browning, U.S. Patent 5 271 965, Thermal Spray Method Utilizing In-Transit Powder Particle Temperatures Below Their Melting Point (Dec. 21, 1993).
5. A.P. Alkhimov, V.F. Kosarev, and A.N. Papyrin: "A Method of Cold Gas-Dynamic Deposition," *Dokl. Akad. Nauk SSSR,* 1990, *315,* pp. 1062-65.
6. A.P. Alkhimov, A.N. Papyrin, V.F. Kosarev, N.I. Nesterovich, and M.M. Shushpanov, U.S. Patent 5 302 414, Gas Dynamic Spraying Method for Applying a Coating (April 12, 1994).
7. R.C. McCune, A.N. Papyrin, J.N. Hall, W.L. Riggs II, and P.H. Zajchowski: "An Exploration of the Cold Gas Dynamic Spray Method for Several Material Systems" in *Thermal Spray Science & Technology,* C.C. Berndt and S. Sampath ed., ASM International, Materials Park, OH, 1995, pp. 1-5.
8. R.C. Dykhuizen, M.F. Smith, D.L. Gilmore, R.A. Neiser, X. Jiang, and S. Sampath: "Impact of High Velocity Cold Spray Particles," *J. Therm. Spray Technol.,* 1998, 8, pp. 559-64.
9. R.C. Dykhuizen and M.F. Smith: "Gas Dynamic Principles of Cold Spray," *J. Therm. Spray Technol,* 1998, *7*(2), pp. 205-12.
10. D.L. Gilmore, R.C. Dykhuizan, R.A. Neiser, T.J. Roemer, and M.F. Smith: "Particle Velocity and Deposition Efficiency in the Cold Spray Process," *J. Therm. Spray Technol,* 1999, *8*(4), pp. 576-82.
11. M.F. Smith, J.E. Brockmann, R.C. Dykhuizen, D.L. Gilmore, R.A. Neiser, and T.J. Roemer: "Cold Spray Direct Fabrication–High Rate, Solid State, Material Consolidation" in *Solid Freeform and Additive Fabrication,* D. Dimos, S.C. Danforth, and M.J. Cima, ed., MRS Symposia Proceedings Vol. 542, Materials Research Society, Warrendale, PA, 1998, pp. 65-67.
12. A.P. Alkhimov, V.F. Kosarev, and A.N. Papyrin: "Gas-Dynamic Spraying, Study of Plane Supersonic Two Phase Jet," *J. Appl. Mech. Tech. Phys.,* 1997, *38*(2), pp. 176-83.
13. A.P. Alkhimov, V.F. Kosarev, and A.N. Papyrin: "Gas-Dynamic Spraying, Experimental Study of the Spray Process," *J. Appl. Mech. Tech. Phys.,* 1997, *38*(2), pp. 183-88.
14. A.P. Alkhimov, V.F. Kosarev, and A.N. Papyrin: "Spraying Current Conducting Coatings On Electro-Technical Units by CGS Methods" in *Tagungsband Conference Proceedings*, E. Lugscheider and R.A. Kammer, ed., DVS Deutscher Verband fur Schweiben, Dusseldorf, Germany, 1999, pp. 288-90.

15. A.P. Alkhimov, A.I. Gulidov, V.F. Kosarev, and N.I. Nesterovich: "Specific Features of Microparticle Deformation Upon Impact on a Rigid Barrier," *J. Appl. Mech. Tech. Physics,* 2000, *41*(1) pp. 204-209.
16. A.P. Alkhimov, S.V. Klinkov, and V.F. Kosarev: "Impingement of a Supersonic Jet of a Rectangular Cut On A Flat Barrier," *Thermophys. Aeromech.,* 2000, *7*(2), pp. 221-28.
17. A.P. Alkhimov, S.V. Klinkov, and V.F. Kosarev: "Study of Heat Exchange of a Supersonic Plane Jet with Obstacle at Gas-Dynamic Spraying," *Thermophys. Aeromech.,* 2000, *7*(3), pp. 375-82.
18. R.B. Bhagat, M.F. Amateau, A.N. Papyrin, J.C. Conway, Jr., B. Strutzman, and B. Jones: "Deposition of Nickel-Aluminum Bronze Powder by Cold Gas-Dynamic Spray Method on 2618 Al for Developing Wear Resistant Coatings" in *Thermal Spray: A United Forum for Scientific and Technological Advances,* C.C. Berndt, ed., ASM International, Materials Park, OH, 1997, pp 361-67.
19. A.E. Segall, A. Nyrin, J.C. Conway, Jr., and D. Shapiro: "A Cold-Gas Spray Coating Process for Enhancing Titanium," *JOM*, 1998, *50*(9), pp. 52-54.
20. H. Kreye and T. Stoltenhoff: "Cold Spray-Study of Process and Coating Characteristics" in *Thermal Spray: Surface Engineering via Applied Research*, C.C. Berndt, ed., ASM International, Materials Park, OH, 2000, p. 419.
21. B. Jodoin: Effects of Shock Waves on Impact Velocity of Cold Spray Particles, pp. 399- *Thermal Spray 2001: New Surfaces for a New Millennium*. C.C. Berndt Ed., K.A. Khor, and E.F. Lugscheider (Eds.), Pub. ASM International, Materials Park, OH-USA, 2001, p. 399.
22. J. Karthikeyan, A. Kay, J. Lindeman, R.S. Lima, and C.C. Berndt: "Cold Spray Processing of Titanium Powder," *Thermal Spray: Surface Engineering via Applied Research*, C.C. Berndt, ed., ASM International, Materials Park, OH, 2000, pp. 255-62.
23. T.H. Van Steenkiste, J.R. Smith, R.E. Teets, J.J. Moleski, and D.W. Gorkiewicz, U.S. Patent 6 139 913, Kinetic Spray Coating Method and Apparatus (Oct. 31, 2000)
24. T.H. Van Steenkiste, J.R. Smith, R.E. Teets, J.J. Moleski, and D.W. Gorkiewicz, U.S. Patent 6 283 386B1, Kinetic Spray Coating Apparatus (Sept. 4, 2001).
25. T.H. Van Steenkiste, J.R. Smith, and R.E. Teets: "Aluminum Coatings Via Kinetic Spray with Relatively Large Powder Particles," *Surf. Coat. Technol.,* 2002, *154,* pp. 237-52.
26. T.H. Van Steenkiste, J.R. Smith, R.E. Teets, J.J. Moleski, D.W. Gorkiewicz, R.P. Tison, D.R. Marantz, K.A. Kowalsky, W.L. Riggs II, P.H. Zajchowski, B. Pilsner, R.C. McCune, and K.J. Barnett: "Kinetic Spray Coatings," *Surf. Coat. Technol.,* 1999, *111,* pp. 62-71.
27. M. Jacobson, A.R. Cooper, and J. Nagy: "Explosibility of Metal Powders," U.S. Bureau of Mines, Washington, DC, RI 5624, 1960.
28. T.H. Van Steenkiste: "Kinetic Spray: A New Coating Process," *Durable Surf., Key Eng. Mater.,* 2001, *197,* Trans Tech Publications, Switzerland, pp. 59-86.
29. J.D. Anderson, Jr., *Modern Compressible Flow,* McGraw-Hill, New York, 1982.
30. C.B. Henderson: "Drag Coefficients of Spheres in Continuum and Rarefied Flows," *AIAA J.,* 1976, *14,* pp. 707-21.
31. D.J. Carlson and R.F. Hoglund: "Particle Drag and Heat Transfer in Rocket Nozzles," *AIAA J.,* 1964, *2,* pp. 1980-84.